Journal of Oceanology and Limnology
Vol. 38 No. 3, P. 665-678, 2020
https://doi.org/10.1007/s00343-019-8370-z

Magnetic properties indicate the sources of hadal sediments in the Yap Trench, northwest Pacific Ocean*

CHEN Yu[1, 2, 4], YANG Jichao[2, **], DADA Olusegun A.[3], YANG Yaomin[2], LIN Zhen[2], CUI Zhen[2], XU Yue[2], YU Hongjun[2], LIU Baohua[2]

[1] *Institute of Deep Sea Science and Engineering*, *Chinese Academy of Science*, *Sanya 572000*, *China*

[2] *National Deep Sea Center*, *Ministry of Natural Resources* (*MNR*), *Qingdao 266237*, *China*

[3] *Dept. of Marine Science & Technology*, *Federal University of Technology*, *Akure 340252*, *Nigeria*

[4] *University of Chinese Academy of Science*, *Beijing 100049*, *China*

Received Dec. 24, 2018; accepted in principle Feb. 18, 2019; accepted for publication Apr. 2, 2019

Abstract Magnetic minerals in marine sediments are often masked by the primary natural remanent magnetization and material source signals. In order to understand sedimentary environment and sources of sediments in the abyss, we studied 126 samples of five bottom surface cores collected by the Jiaolong Submersible at 4 000–7 000 m in depth during the third stage of the China's 38th Ocean Voyage. The magnetic properties of the sediments were analyzed using Thermosusceptibility (*k*-*T*) curves and Day plot. The results show that the magnetic minerals in the sediments of the Yap Trench are mainly maghemite, and the overall magnetic and soft magnetic properties were strong. The magnetic particles of sediments are dominated by pseudo single domains (PSD) grains. The main source of sediment is locally-derived basalt debris and volcanic debris, and the process of sedimentation is gravity-like flow deposition.

Keyword: magnetic property; material resource; hadal sediment; Yap Trench

1 INTRODUCTION

Environmental magnetism has been widely used to investigate the formation, transportation, deposition, and post-depositional alterations of magnetic minerals under the influences of a wide range of environmental processes (Liu et al., 2003). Environmental magnetic susceptibility method is used because it is simple, fast, efficient, repeatable, and non-destructive to samples (Evans and Heler, 2003; Kars et al., 2017) whether in loess (e.g. Ghafarpour et al., 2016; Guan et al., 2016), lake sediments (Oldfield, 1994; Roza et al., 2016; Kirscher et al., 2018), deep sea sediments (Dong et al., 2016; Lund et al., 2017), or core (Dura et al, 2015; Yang et al., 2016).

Little is known about the subduction zone, especially the abyss that exceeds 6 000 m water depths until human exploration of the abyss began with the invention of echo-sounding technology for submarine detection in the late 19th and 20th centuries (Pautot et al., 1987). In the last 50 years, a series of geological surveys (Kitahashi et al., 2014) in the Mariana Trench and the Puerto Rico Trench have revealed the importance of the Earth system processes such as deep ocean circulation and deep cyclone circulation (Jamieson et al., 2009). They have not only revealed large number of material inputs, rich biodiversity at this great depth but also shown a unique sedimentary environment characterized by high pressure, low temperature, and frequent seismic activity (Gallo et al., 2015).

At present, there are few studies on the use of magnetic susceptibility to investigate the material source and sedimentary environment of the trench. Kawamura et al. (2008) analyzed seven columnar

* Supported by the National Basic Research Program of China (973 Program) (No. 2015CB755901), the Taishan Scholar Project Funding (No. tspd2016007), the 13th Five-Year Plan Program of the China Ocean Mineral Resources Research and Development Association Research (No. DY135-S2-2-08), the China Postdoctoral Science Foundation (No. 2017M610403), and the National Key R&D Program of China (Nos. 2018YFC0309802, 2018YFC0309903)
** Corresponding author: yangjichao.1@163.com

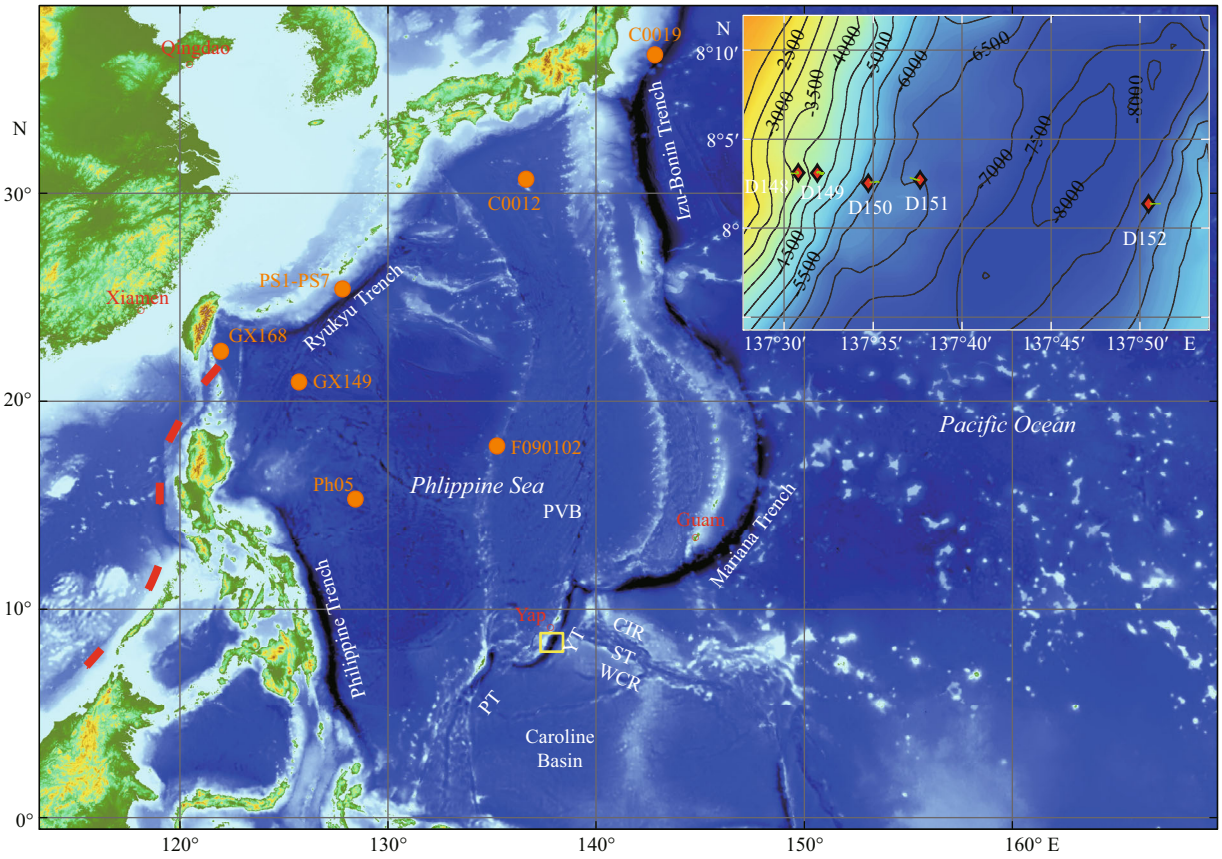

Fig.1 The location of the Yap Trench area

Marked by the Core F090201 from the East Philippine Sea; Cores GX149 and GX169 from the West Philippine Sea (Li et al., 2006, 2015); Core C0012 from the Shikoku Basin (Kitajima and Saffer, 2015); Core PS1-PS7 from the Ryukyu Trench (Kawamura et al., 2008); and Core C0019 from the Japan Trench (Yang et al., 2016). The upper right corner is sampling position distribution map of Core D148, D149, D150, D151 and D152 in the yellow frame area (Yang et al., 2018).

samples from the Ryukyu Trench and found that the magnetic carriers of the sediments were mainly magnetite and maghemite, containing a small amount of hematite. The magnetic mineral content at the top of the sediment was terrigenous debris. Both results of the magnetic and geochemical analyses proved that fine-grained magnetic minerals dissolved with increasing burial depth in anoxic environment. In addition, in the core from the Japanese Trench, magnetic susceptibility was used to correlate the different sliding surfaces of the earthquake, in order to reveal the cumulative effects after several earthquakes (Yang et al., 2016).

Located in the southeastern part of the Philippine Sea, the Yap Trench forms the southeastern boundary of the Philippine Plate with the Izu Ogasawara Trench, the Mariana Trench, and the Palau Trench (Fig.1). The Yap Trench is 700 km long and has a curved shape that protrudes southeastward. The water depth of the Yap Trench is between 6 000 and 9 000 m and the maximum water depth is 8 946 m (10°29.957′N, 138°40.987′E) (Fujiwara et al., 2000). The magnetic characteristics of the sediments in the Yap Trench are still unknown. In this paper, five magnetic core samples obtained, by the Jiaolong Manned Submersible, from the Yap Trench were used to carry out environmental magnetism and sedimentological studies to reveal the magnetic properties of the Yap Trench. In addition, the mineral species and distribution characteristics, the role of environmental magnetic properties of the source of sediments in the Yap Trench were explored.

2 MATERIAL AND METHOD

During the 38th Ocean's Voyage of the Chinese Research Vessel, *Xiangyanghong 09*, from June 4–13, 2017, five deep push core samples (Core D148, D149, D150, D151, and D152) of sediments were collected by using manned submersible Jiaolong in the southern Yap (Fig.2, Table 1).

As the Fig.2 and video records show, the substrate of site D148, D149, and D150 mainly are deep sea

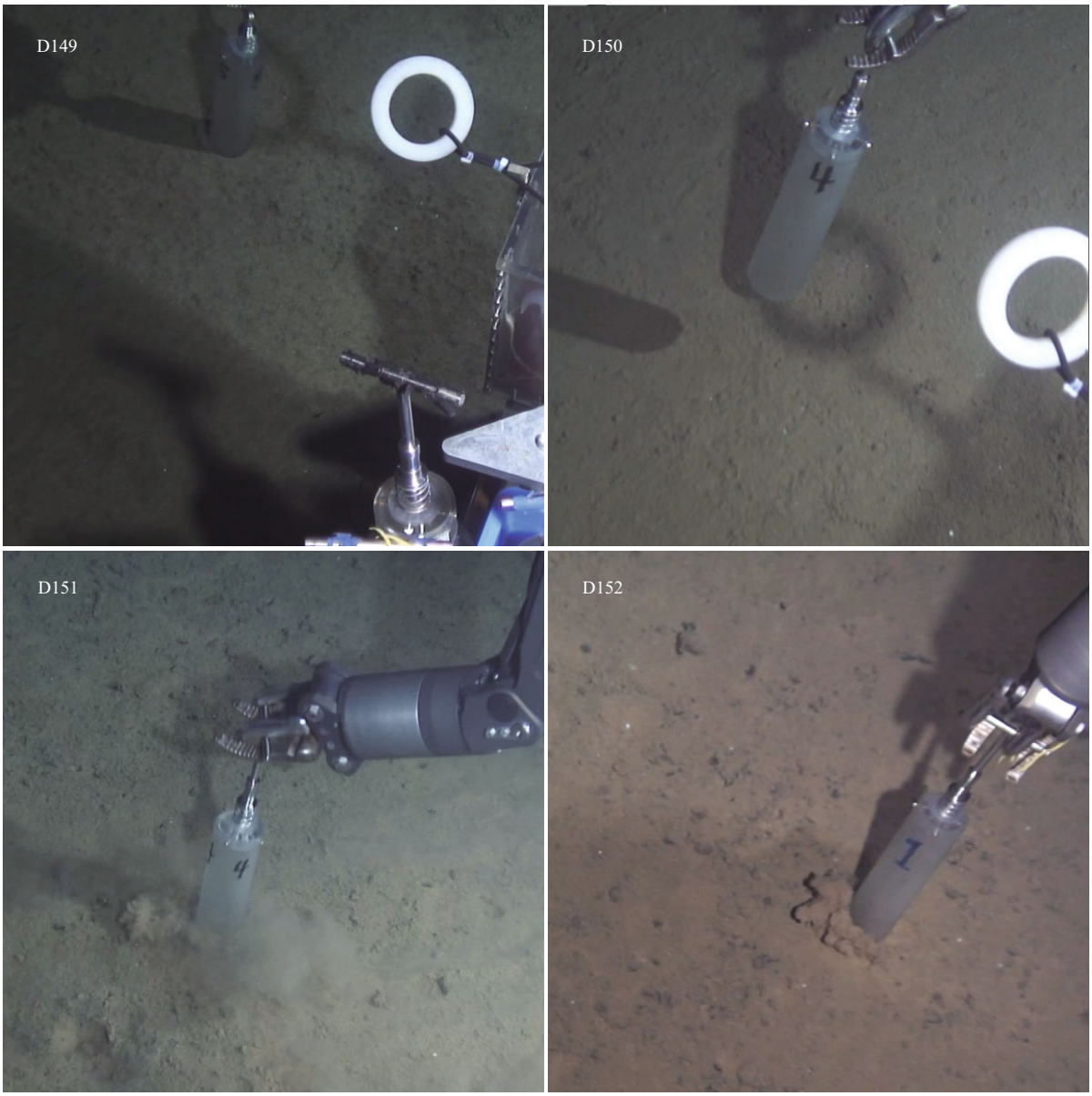

Fig.2 Sediment sampling environment in the Yap Trench

All pictures were taken from the video screenshots recorded by the manned submersible Jiaolong. Because of the camera failure, dive 148 could not capture photos and videos (Yang et al., 2018).

Table 1 Specifications of the cores sampling in the Yap Trench

Core ID	Latitude (°N)	Longitude (°E)	Deep (m)	Sample length (cm)	Sampling method
D148	8.058 4	137.523 3	4 161	24.5	Push core
D149	8.055 8	137.548 2	4 993	20	Push core
D150	8.050 9	137.589 0	6 173	30	Push core
D151	8.031 0	137.569 3	6 582	24	Push core
D152	8.023 0	137.843 4	6 682	28.5	Push core

clay and a large number of gravel, while that of site D151 and D152 are largely compried of deep sea clay. The same situation was found in our cores (Fig.3), there are many debris in the middle of D149, D150, and the bottom of D152. The dopsit thickness of D148, D149, and D150 are also thinner than that in site D151 and D152.

We analyzed 126 samples by segmenting each core at 1-cm interval. The samples were dried at 50°C, and then ground into a powder with an agate mortar. About 3 g of each sample was crushed and wrapped in a polyethylene cling film and placed in a 4.74-cm^3 plastic cube, crushed and prepared for analysis. The magnetic measurements were carried out at the Environmental Magnetics and Paleomagnetic Laboratory of the Third Institute of Oceanography,

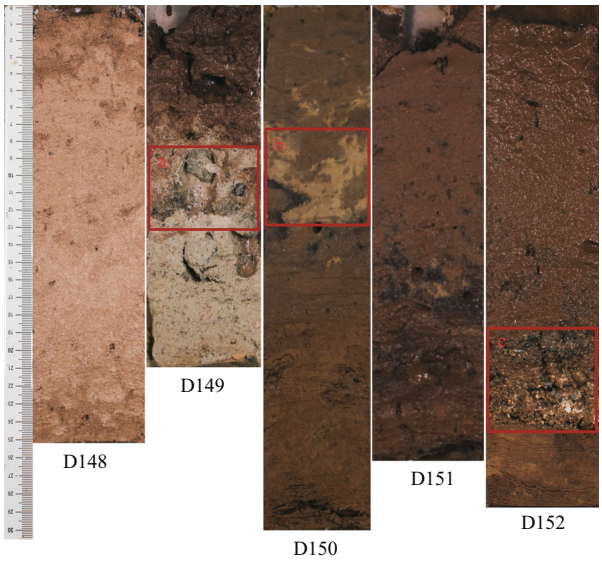

Fig.3 The photograph of cores in Yap Trench

Red frame a, b and c are debris that contains gravel and grit.

Ministry of Natural Resources, China.

All samples expressed on a mass-specific basis, with low (976 Hz) and high (15 616 Hz) frequency magnetic susceptibilities (χ_{lf} and χ_{hf}, respectively), were measured using an MFK1-FA Multi-Function Kappabridge susceptometer (AGICO, Brno, Czech Republic) with a detection limit of 2×10^{-8} SI and a measurement accuracy of 0.1 percent, at a field intensity of 200 A/m (peak-to-peak). χ_{lf} was taken as the mass-specific low-field magnetic susceptibility (χ).

The isothermal remanent magnetization (IRM) and anhysteretic remanent magnetization (ARM) were selected by JR-6A rotating magnetic force, pulse magnetizer and DTECH2000 alternating demagnetizer. The procedure for the remanent magnetization measurements are is as follows: first, the samples were placed at the peak of alternating magnetic field of 100 mT and a DC magnetic field of 0.002 5 mT to obtain a non-hysteresis remanent magnetic ARM. Then isothermal remanent $IRM_{40\ mT}$, $IRM_{100\ mT}$ and $IRM_{300\ mT}$, respectively, were obtained for samples with 40 mT, 100 mT, 300 mT after demagnetization; finally, the saturated isothermal remanent magnetization (SIRM) was obtained for the 2T magnetic field.

Magnetic hysteresis loops and back-field isothermal remanent magnetization curves were measured to determine the hysteresis parameters, coercive force (H_c), remanence coercive force (H_{cr}), saturation remanence (M_{rs}) and saturation magnetization (M_s) using a MicroMag Model 3900 vibrating sample magnetometer (VSM, Princeton Measurements Corp.). The maximum applied field was 2.0 T.

Frequency dependence of the magnetic susceptibility (χ_{fd}%), SOFT, SIRM/χ and S ratio (S_{300}), were calculated as follow:

$$\chi_{fd}\%=[(\chi_{lf}-\chi_{hf})/\chi_{lf}]\times100,$$

$$SOFT=(SIRM-IRM_{40})/2,$$

$$SIRM/\chi=SIRM/(\chi_{lf}\times100),$$

$$S_{300}=IRM_{300}/SIRM.$$

The *k*-*T* measurement of 6 representative samples was completed with a MFK1-FA Kappabridge susceptometer operating at a field of 200 A/m and a frequency of 976 Hz with a CS-4 high-temperature furnace attached to it. Samples were heated to 700°C in argon of standard laboratory quality (the flow rate was about 100 mL/min) with a heating rate of approximately 6°C/min, and subsequently cooled at room temperature.

The Yap sediment particle size analysis was performed using the Malvern 2000 particle size analyzer at the Geology Laboratory of the First Institute of Oceanography, Ministry of Natural Resources, China. Firstly screening the gravel and very coarse particles (>2 000 μm) in the samples, dilute hydrochloric acid was used to break down calcium carbonate and then to be washed out, 2 g of each sample was analyzed to obtain the particle size data. The average particle size (Md) was calculated based on the analysis results.

3 RESULT

3.1 Particle size analysis

The average particle size (Md) of Yap Trench samples range from 5.59 Φ to 7.92 Φ, the mean value is 7.01 Φ, relatively fine but generally large variation. The Md of Cores D148–D152 is 6.73 Φ, 6.89 Φ, 7.15 Φ, 7.32 Φ, 6.68 Φ, respectively. Among these, the particle size of Core D149 has the largest variation with changing depth, nearly 2 Φ. The particle sizes of Cores D148 and D149 are coarsen along down-core while that of Cores D148 and D149 are fine along down-core. There are no significant correlations between particle size and magnetic parameters (Fig.4).

3.2 Remanent magnetization and hysteresis parameters

The results of each magnetic parameter analysis and its range of variation are shown in Table 2. The distributions of χ, SIRM, and SOFT are more dispersed, and their σ are larger ($>23\times10^{-8}$ m^3/kg, $>850\times10^{-6}$ Am^2/kg, $>334\times10^{-6}$ Am^2/kg, respectively).

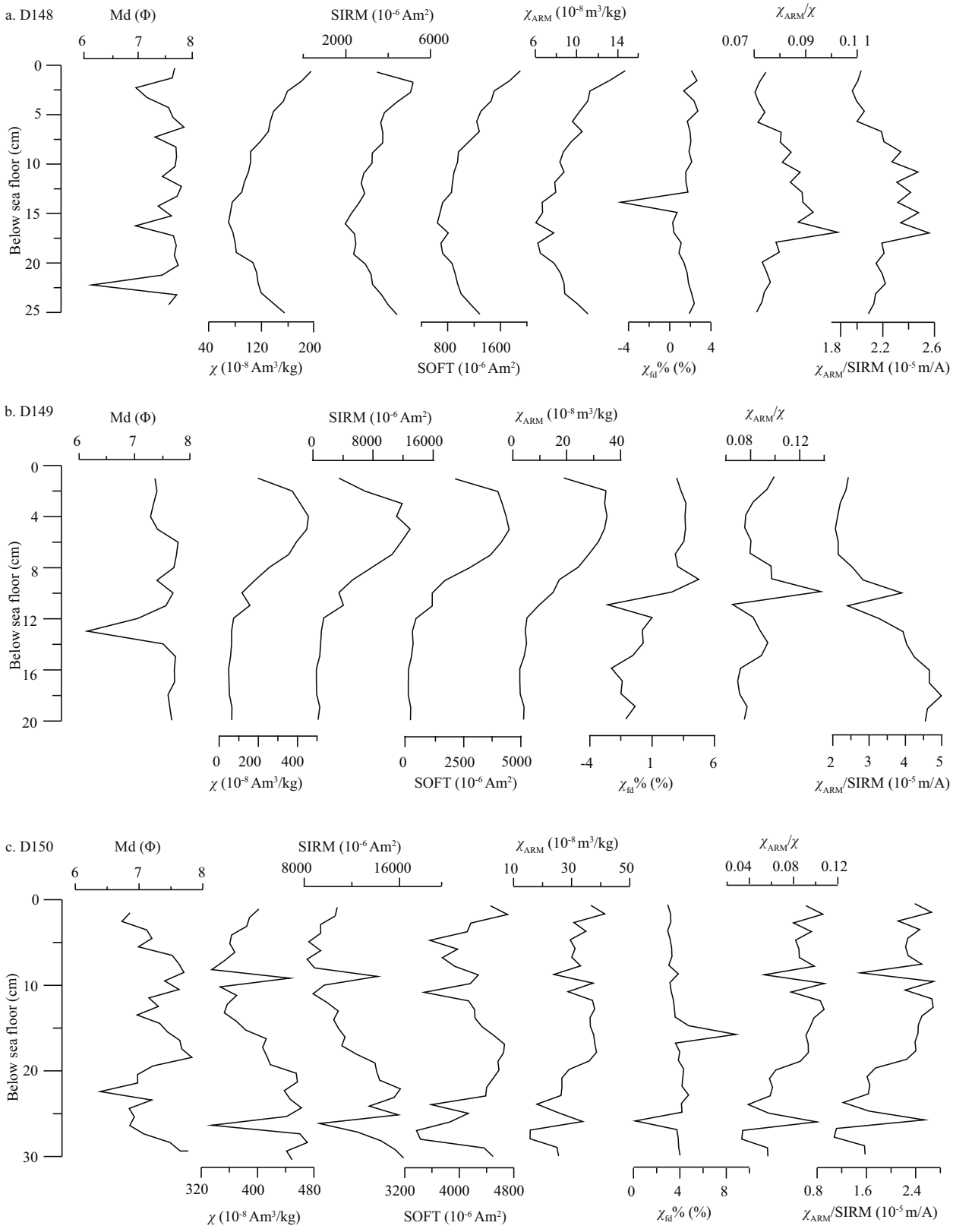

Fig.4 The average particle size (Md), χ (10^{-8} m^3/kg), SIRM (10^{-6} Am^2/kg), SOFT (10^{-6} Am^2/kg), χ_{fd}% (%), χ_{ARM} (10^{-8} m^3/kg), χ_{ARM}/χ, χ_{ARM}/SIRM values of the Yap Trench sediments

To be continued

Fig.4 Continued

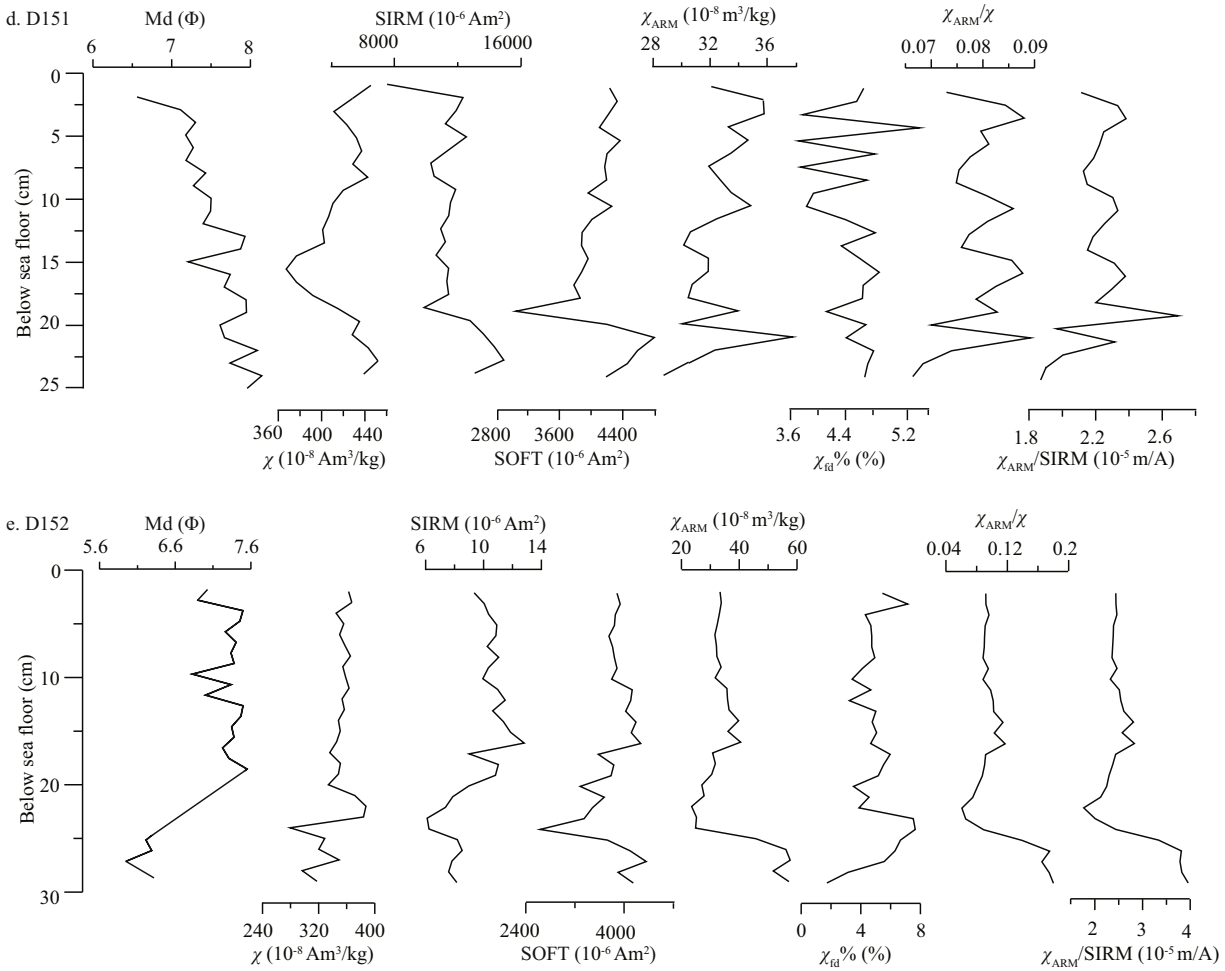

The maximum values of χ, SIRM, and SOFT appear at the bottom of the Core D150 (Fig.4). The χ, SIRM, and SOFT exhibit high values in the Core D150, D151, and D152, from the abyss deeper than 6 000 m, and the variation is not large (relative small σ). The remanent magnetic parameters of the Core D148 and D149 display lower values. The values in the Core D149 varied significantly, showing distinct features that display low values at the bottom (Fig.4). The overall trends of χ, SIRM, and SOFT in the Yap sediments are very consistent in the downcore and between cores. The correlations between them have always been used to indicate types of magnetic mineral in lots of research.

The mean χ_{fd}% of the Yap Trench is 3.21%, the χ_{fd}% of Core D148 and D149 is relatively lower (mean value are 1.25% and 0.74%). The variance of χ_{fd}% in Core D149 is the largest (σ=2.26%), while the χ_{fd}% of Core D150 and D151 are relatively stable and above 2%. The mean χ_{fd}% of Core D152 is the highest and its χ_{fd}% has a relatively distinct variation at the bottom.

As shown in Fig.4 and Table 2, there are resemblance in the χ_{fd}%, χ_{ARM}, χ_{ARM}/χ, χ_{ARM}/SIRM of the Yap Trench. Each magnetic parameter of Core D148 is relatively small. The magnetic parameters of Core D149 is the largest in Yap Trench sediments, while those of Core D149 and D150 are actually smaller. In general, the variance of χ_{fd}%, χ_{ARM}, χ_{ARM}/χ, and χ_{ARM}/SIRM are relatively consistent and presented an increasing trend towards the deep trench. It is worth noticing that there are no significant correlations between particle size and magnetic parameters, indicating that study area probably happened sedimentary disturbance, and mixing in large-scale.

The *k*-*T* cycles heated from room temperature to 700°C of representative samples are shown in Fig.5. On the heating branches, *k* gradually increases up to approximately 300°C, then is stable from 300°C to 400°C. This might have resulted from the transformation of some magnetic minerals into weak magnetic hematite, as it decreased dramatically to nearly zero at about 700°C. The cooling *k*-*T* cycles

Table 2 The magnetic characteristics of sediments in the Yap Trench

		D148	D149	D150	D151	D152
χ (10^{-8} m^3/kg)	Max	197.544	455.42	470.72	452.02	387.54
	Min	69.42	48.17	334.89	367.28	279.38
	Mean	117.69	199.68	402.89	417.36	346.86
	σ	34.35	150.74	42.71	23.07	22.97
SIRM (10^{-6} Am^2/kg)	Max	5.19×10^3	12.52×10^3	16.33×10^3	14.91×10^3	12.81×10^3
	Min	1.90×10^3	0.70×10^3	8.25×10^3	7.55×10^3	6.10×10^3
	Mean	3.32×10^3	5.02×10^3	11.90×10^3	11.62×10^3	9.63×10^3
	σ	0.85×10^3	4.23×10^3	2.56×10^3	1.50×10^3	1.70×10^3
SOFT (10^{-6} Am^2/kg)	Max	1.94×10^3	4.64×10^3	4.71×10^3	4.80×10^3	4.33×10^3
	Min	653.44	207.92	3.37×10^3	3.05×10^3	2.60×10^3
	Mean	1.10×10^3	1.94×10^3	4.16×10^3	4.10×10^3	3.78×10^3
	σ	334.16	1.76×10^3	383.23	330.88	3.43×10^3
χ_{ARM} (10^{-8} m^3/kg)	Max	14.72	35.26	41.40	37.79	57.64
	Min	6.05	3.53	15.65	28.73	23.55
	Mean	9.17	16,86	30.64	32.64	36.33
	σ	2.09	12.39	6.79	2.15	93.07
χ_{fd}% (%)	Max	2.73	4.16	8.84	5.48	7.65
	Min	-4.76	-3.04	0.16	3.72	1.72
	Mean	1.25	0.74	3.80	4.49	4.92
	σ	1.40	2.26	1.24	0.43	1.33
χ_{ARM}/χ	Max	0.10	0.14	0.11	0.09	0.18
	Min	7.04×10^{-2}	6.72×10^{-2}	3.32×10^{-2}	6.55×10^{-2}	6.08×10^{-2}
	Mean	8.02×10^{-2}	8.72×10^{-2}	7.79×10^{-2}	7.80×10^{-2}	0.11
	σ	7.97×10^{-3}	1.46×10^{-2}	2.22×10^{-2}	0.62×10^{-2}	3.17×10^{-2}
χ_{ARM}/SIRM (10^{-5} m/A)	Max	2.56	4.89	2.69	2.69	3.97
	Min	1.96	2.10	1.08	1.86	1.78
	Mean	2.21	3.30	2.07	2.21	2.66
	σ	0.16	1.00	0.49	0.18	0.56

have two patterns: one pattern as D148-2, D149-12, D150-1, D151-2. Here, k increase sharply as temperature decreased from 700°C to 300°C, and at the same time higher than the same temperature during heating. As temperature decreased from 300°C to the room temperature, the values of k decrease slowly and become steady. The other pattern as D149-3 and D152-3. Here, the values of k increase distinctly as the temperature decreased from 700°C to 350°C and at the same time even lower than the same temperature during heating.

The M_{rs}/M_s and H_{cr}/H_c ratios (Day plot) of the Yap Trench sediments are mainly located in the PSD (pseudo-single-domain) region, between two SD (single-domain)+MD (multi-domain) mixing curves of Dunlop and Özdemir (2001).

4 DISCUSSION

4.1 Inference from Environmental magnetism

In the present study, χ and SIRM have been used to reflect the content of magnetic minerals. The distributions of χ, SIRM and SOFT are shown in Fig.4. As can be seen, magnetic minerals of Yap Trench sediments are mainly concentrated in the Cores D150, D151 and D152 and the middle of D149. Among these, the magnetic minerals content of Core D150 is the highest. As shown in Fig.6a, the SIRM of Yap Trench sediments correlates well with χ (R^2=0.97). On the one hand, sediments have magnetic uniformity, and on the other hand, χ can be used as an indicator for representing magnetic minerals. The magnetic strength of magnetite is several orders of magnitude

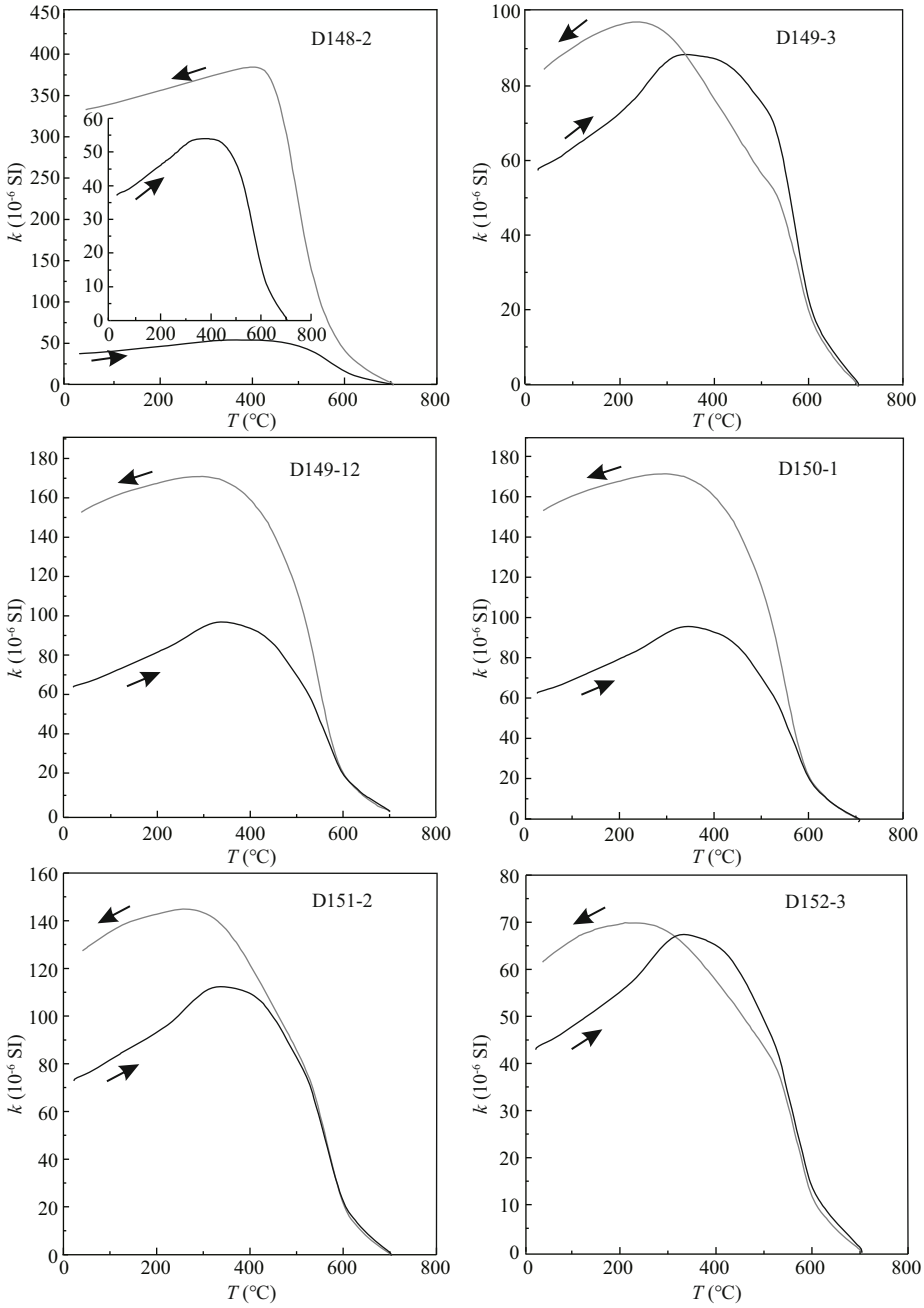

Fig.5 The *k*-*T* cycles of representative samples collected from the Yap Trench

The black lines are heating cycles and grey lines are cooling cycles, the arrows direct the trend of temperature change.

higher than that of hematite. Therefore, in this study, χ is used as an indicator of the level of magnetite in the sample. SIRM and SOFT differ in mineral directivity: SIRM is mainly affected by ferrimagnetic minerals and incomplete antiferromagnetic minerals, but not by paramagnetic minerals and diamagnetic minerals, while SOFT is mainly affected by ferrimagnetic mineral (Liu et al., 2010). The correlation between SIRM and SOFT is R^2=0.99, which indicates that the magnetic properties of the Yap Trench sediments are dominated by ferrimagnetic minerals, and the contribution of incomplete antiferromagnetic minerals is limited. As shown in Fig.6a, the incomplete diamagnetic minerals in the Core D148 and D149 samples are relatively higher than others, while the D150, D151, D152 ferrimagnetic minerals are relatively higher. The SIRM value is the largest among the SD minerals and zero in the SP minerals. The SIRM distribution of the Yap Trench indicates that the magnetic domains of the three sites in the ultra-abyss are finer, and the number of SD magnetic particles is more than that of D148 and

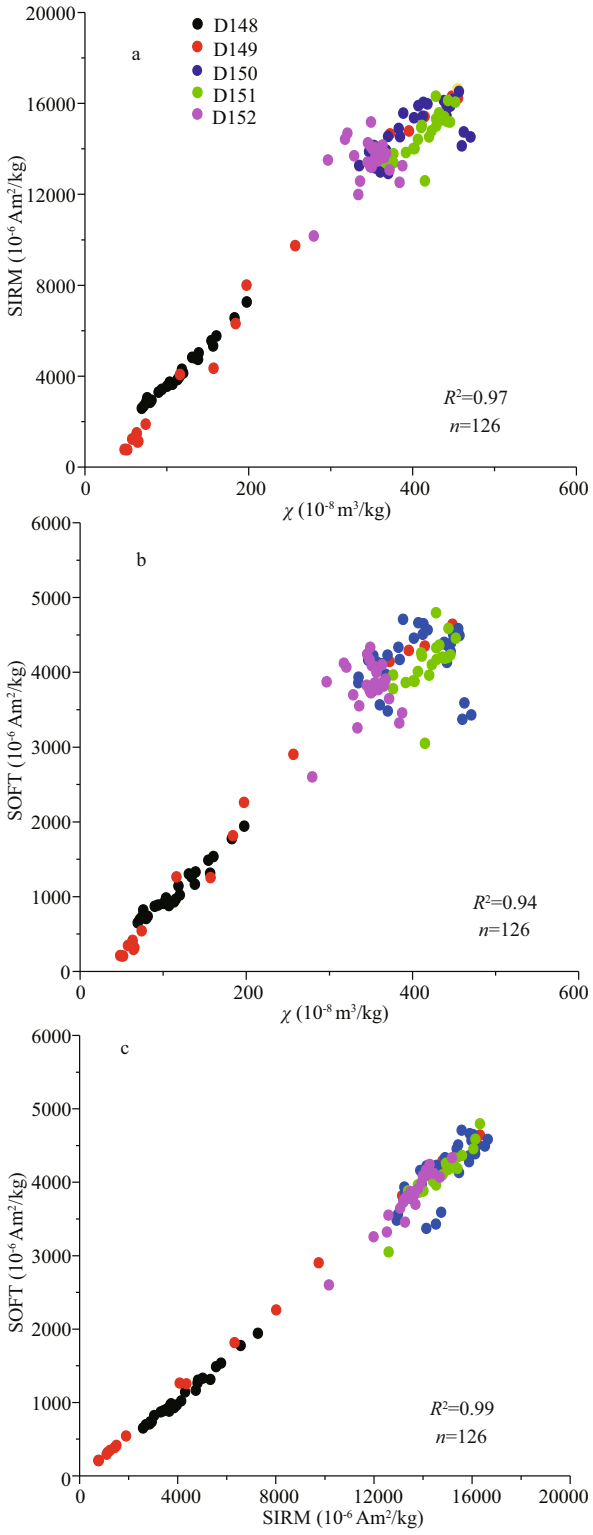

Fig.6 The correlation between χ, SIRM and SOFT

D149. Unlike other studies that particle size has significant correlation with magnetic parameters (Liu et al., 2007; Prajith A et al., 2015), the particle size of sediments in Yap Trench has different trend from magnetic parameters, showing that there probably happened sedimentary disturbance and mixing in large-scale.

The *k*-*T* cycles can be used to effectively determine the type of magnetic mineral (Dunlop et al., 1997; Geissman, 2004). For instance, maghemite is usually transformed into weakly magnetic hematite at the temperature that ranges from 300°C to 400°C. Temperature between 400°C and 590°C is the unblocking temperature when maghemite is heated to Curie temperature and *k is* distinctively decreased. At 700°C is the Curie temperature of maghemite when *k* is closed to 0 (Thompson and Oldfield, 1995). As shown in Fig.5, all these characteristics prove that the maghemite is the main mineral in Yap Trench sediments. During the cooling process, the *k* value increases as the temperature decreased from 590°C to 430°C, but this temperature range is larger for the *k* value during heating, indicating that magnetite is formed during the heating process. We observed that the phase characteristics of the *k*-*T* cycle are consistent with the maghemite in the deep-sea basalt of the drilling report of Riisager et al. (2002). In summary, the mineral composition of the Yap Trench sediments is dominated by ferrimagnetic maghemite, containing a small amount of antiferromagnetic hematite and ferromagnetic magnetite.

4.2 Magnetic domain characteristics of sediments in Yap Trench

Generally, the magnetic domain structure of magnetic minerals can be subdivided into SP, SD, PSD and MD grains from fine to coarse (Liu, 2010).

χ_{fd}% can reflect the contribution of fine-viscous SP particles near the SP and SD boundaries to the magnetic susceptibility. When χ_{fd}%<2%, the sample is basically free of SP particles. But when χ_{fd}%>5%, it indicates there are more SP particles in the sample (Maher and Thompson, 1999). The overall average χ_{fd}% is 3.21%, further indicating that the SP particles in these sediments are very low. The Cores D148 and D149 sediments are basically below 2% (Mean 1.25% and 0.74%) indicating that there are few SP particles at the top of Core D148, which are basically free of SP particles (Fig.7).

The χ_{ARM} has high sensitivity to SD crystals. The high value of χ_{ARM} in the Yap trench sediments appears in the super abyss, and at the higher-position sites are relatively low, indicating that the sediments in the deep trenches have high SD particles. χ_{ARM}/χ is commonly used to indicate the grain size of ferrimagnetic minerals. Low values reflect more MD

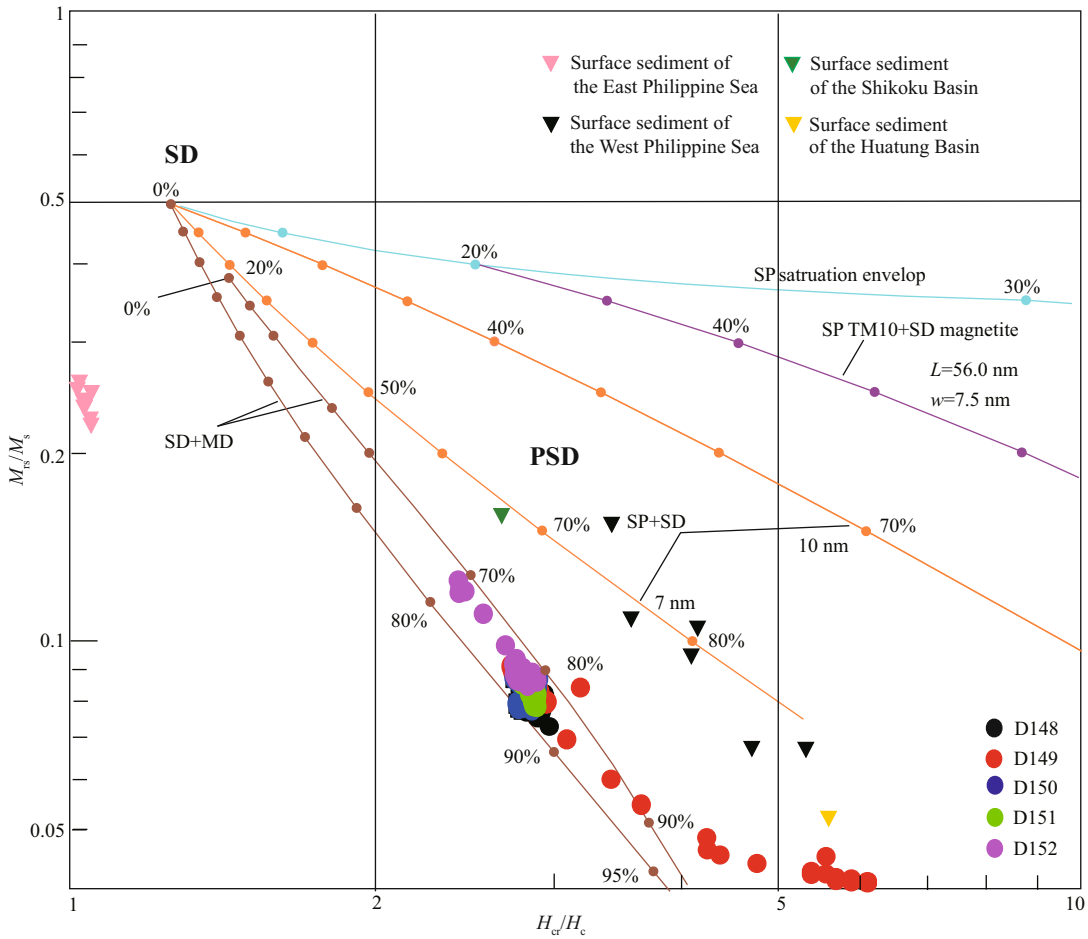

Fig.7 Day plot of the hysteresis ratios M_{rs}/M_s and H_{cr}/H_c ratios of core sediments

Single-domain (SD), multi-domain (MD) and pseudo-single-domain (PSD) boundaries are after Dunlop and Özdemir (2001). Numbers adjacent to curves are volume fractions of the soft component (super-paramagnetic, SP or MD) in mixtures with SD grains. The pink triangle, dark green triangle, black triangle and yellow triangle represent surface sediments from the East Philippine Sea (Meng et al., 2006), Shikoku Basin (Kitajima and Saffer, 2015), West Philippine Sea (Li et al., 2015) and Huatung Basin (Yang et al., 2016), respectively.

and SP grains, while high values indicate more single domain particles. The χ_{ARM}/SIRM is extremely limited by SP, and the low value reflects the coarser MD grain content (Kim et al., 2013). As illustrated in Fig.4, the χ_{ARM}/χ and χ_{ARM}/SIRM of the Yap Trench are small, with average values of 8.57×10^{-2} and 2.43×10^{-5} m/A, respectively (Table 2), less than the standard χ_{ARM}/χ>10, χ_{ARM} /SIRM>60×10^{-5} m/A, indicating that the ferrimagnetic mineral grains in the Yap Trench sediment are mainly coarser PSD.

The Day plot can visually reflect the magnetic domain information of ferrimagnetic minerals (Day et al., 1977; Dunlop and Özdemir, 2001). We calculated the M_{rs}/M_s and H_{rc}/H_c based on the hysteresis loop measurements using the MicroMag 3900 (Fig.7). As shown in Fig.7, the sediment samples of the Yap Trench basically fall in the PSD region, and based on the magnetic domain boundary curve of Dunlop and Özdemir (2001), the hysteresis loop of the Yap sediment mainly falls on the SD+MD mixing curves within the range of 70%–90%. This is basically consistent with the previous χ_{ARM} and χ_{fd}% indicator analysis results. In addition, Figure 7 shows the distribution of M_{rs}/M_s and H_{rc}/H_c in other surface columnar sediments of the Philippine Seas. It is found that the core magnetic domain characteristics of the West Philippine Sea and the Shikoku Basin are similar to those of the Yap Trench, mainly, falling within the range of 75%–90% of SP (7 nm)+SD mixing curves.

4.3 Source of sediments from their magnetic characteristics

The factors affecting the source of sediment are mainly debris forces, biological forces, dust sedimentation and early diagenesis, etc. The use of magnetic properties to analyze the source of sediment must clarify the genesis of minerals in sediments because only the magnetic minerals of debris has

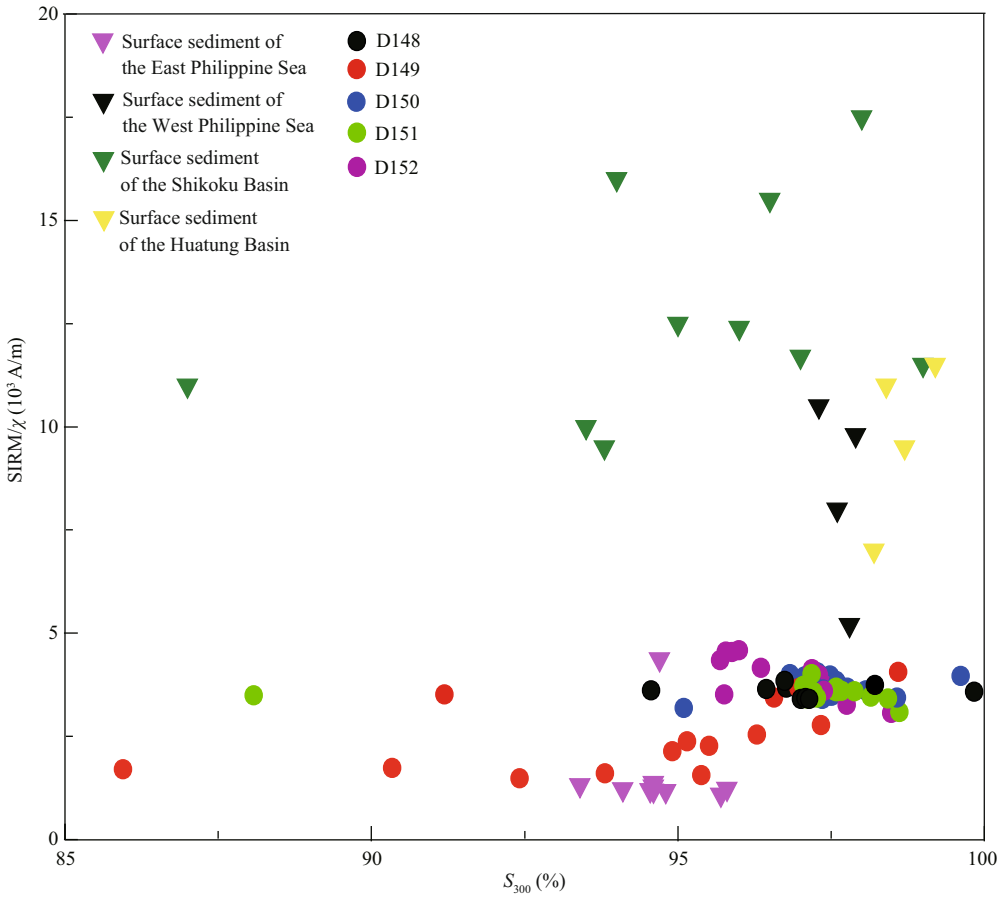

Fig.8 Comparison SIRM/χ and S_{300} of the Yap Trench sediments with those parameters of the East Philippine Sea (Meng et al., 2006), Shikoku Basin (Kitajima and Sahher, 2015), West Philippine Sea (Li et al., 2015) and Huatung Basin (Yang et al., 2016)

information about the source. The formation of biological forces in early diagenesis may not represent the original magnetic characteristics (Canfield et al., 2006; Sim et al., 2011; Li et al., 2016). Biological forces are usually accompanied by early diagenesis. Under the Sulfate-reducing bacteria, pyrite is formed, of which melnikovite and pyrrhotite are intermediate products. So, in the hadal sediments that under reduction environment, pyrite can be regarded as an indication of biological forces (Novosel et al., 2006; Borowski et al., 2013). The SIRM/χ of the melnikovite-bearing samples is often greater than 80 kA/m (Dewangan et al., 2013), while the SIRM/χ values of the Yap Trench sediments are between 1.48 and 4.58 kA/m, and the parameters such as the *k-T* cycle do not reflect the inclusion. Information on melnikovite and pyrrhotite can be considered to be unaffected by biological forces. Early diagenesis will dissolve low coercivity minerals (ferromagnetic minerals), resulting in a rapid decline in S_{300}. Low coercivity minerals and high coercivity mineral ratios decrease (Liu et al., 2007) with large SOFT values. The magnitude is decreasing. It can be seen from Figs.6 & 8 that this phenomenon does not exist in Yap Trench sediments, which proves that the Yap Trench sediments is largely unaffected by the early diagenesis, and the magnetic mineral preserves the information of the original sediment. The SIRM/χ, *k-T* cycle, and SOFT indicate that the sediment is mainly low-coercivity magnetite, while the generally higher S_{300} value and low HIRM indicate that there are few hard magnetic minerals, such as hematite and goethite, in the sediment. The main source of hard magnet minerals in marine sediments is dust, so there are few wind and dust deposits in the Yap Trench. Combined with the previous analysis, it can prove that the Yap Trench sediments are mainly debris sources. Not only that, by comparing SIRM/χ and S_{300} of Yap Trench with these of other places, we can further determine the resource of sediment in the Yap Trench.

In our study, the sedimentary magnetic properties of the study area are compared with those in the surface column of the Core F090201 from the East Philippine Sea (Meng et al., 2006), Core GX149 from

the West Philippine Sea (Li et al., 2015), and the Core GX168 from the East China Sea Basin (Li et al., 2016); and also with sediment at the top of C0012 core from the Shikoku Basin. As shown in Fig.8, the D149 lower layer sediment is very close to the magnetic characteristics of the Core F090201 from the East Philippine Sea, while the magnetic characteristics of the Cores D150, D151, and D152 from the Yap Trench sediments are relatively close to the Core GX149 from the West Philippine Sea and the Core GX168 from the East China Sea Basin surface. It is worth noting that the relationship between M_{rs}/M_s and H_{cr}/H_c (Day plot) of the Core GX168, the Core GX149 and the Yap trench sediment are very close (Fig.7). With reference to similar magnetic characteristics, the characteristics of χ, SIRM, and SOFT are lower than those of the high coercivity hematite content of the volcanic debris. The volcanic debris are mainly from the Philippine island and caused by currents and the volcanic material debris of the nearby Mariana Trench. The Core GX149 sediments from the Western Philippine Sea are greatly affected by dust deposits, which are inconsistent with the situation in the Yap Trench. The turbidity developed in the Core GX168 from the Huatung Basin are very similar to the Yap Trench sediments in terms of sedimentary magnetic mineral types, *k*-*T* cycle, and SIRM/*x* characteristics and stratification characteristics.

SIRM-χ scatter plot for Cores D148 and D149 from the Yap Trench are significantly different from other sites, indicating that the source composition is different. Dots of Core D149 are disperse, indicating that there are many debris, large particle size variations, and magnetic domain MD crystallites. More important, the abnormally high value of the χ in the middle of the core indicates that the sedimentary environment has changed greatly (Fig.4). The upper color of Core D149 is lighter than the lower part, the sand is thick, and the silt clay has a small specific gravity, exhibiting homologous turbidity characteristics (Bridge and Demicco, 2011).

Figure 9 illustrates plot the C-M map of the sandstone-like granularity data of the Yap Trench sediments and the linear distribution characteristics of the gravity flow. The slope and position of the sediments are different, and the overall gravity flow characteristics are atypical. Among these, the gravity flow characteristics of the Core D149 are more significant. We infer that it may be that the deep-sea basalt is broken at 4 000 m (D148), and the

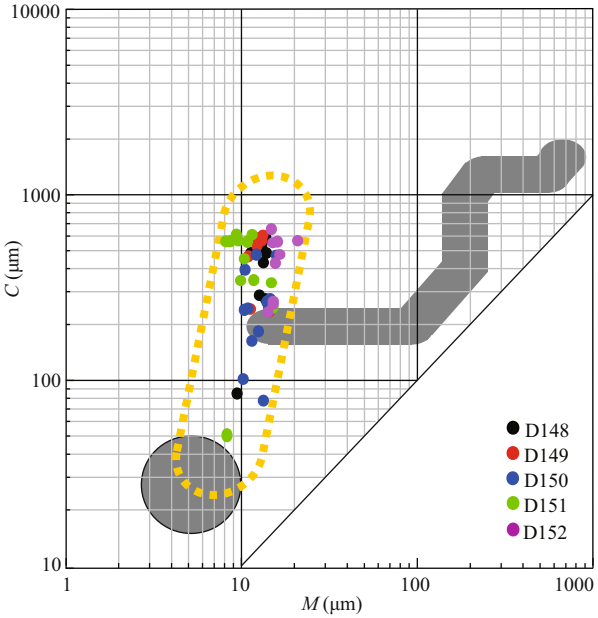

Fig.9 C-M map of the Yap Trench sediment, in which the circular shadow is the oceanic suspended sediment

The round shadow is the range of pelagic suspensions, and the upper banding shadow is the range of shelf and slope sediment.

sedimentation occurred after the turbidity of the coastal gully at 4 500 m (D149), covering the volcanic clastic sediments deposited by current before the sedimentation site. This situation is consistent with that there are no significant correlations between particle size and magnetic parameters.

Turbidity current is very similar to the conditions generated by gravity flow: sufficient water depth, sufficient material, necessary slope, and trigger mechanism. The first two are the source of matter, and the third is the source of turbidity (Li et al., 2016; Jiang, 2010). In the marine environment, the main stream occurs mostly in the deep-sea area such as the seabed valley. The trigger mechanism includes sea level fluctuations, earthquakes, volcanic eruptions, storm surges, etc., causing loose deposits on steep terrain to mix down the slope, thereby forming a turbid stream (Arai et al., 2013). Cores D148 and D149 are located on the steep slope of the west side of the Yap Trench at 4 000 m and 4 500 m depths, respectively. They are close to the magma eruption of the Mariana Trench and close to the volcanic seismic belt, thereby providing a rich source of material and favorable terrain for gravity flow development.

In summary, the main sources of sediments in the Yap Trench are nearly-source clastics and volcanic debris. The Core D150, Core D151, Core D152, and the upper layers of Cores D149 is the deposition of

basalt and diabase debris, which is triggered by earthquakes and volcanic eruptions. The sediments are mainly composed of terrestrial material debris such as basalt and pyrozenite. The Core 148 and the bottom of Core D149 are mainly volcanic dust and debris.

5 CONCLUSION

The magnetic minerals in the surface columnar sediments of the Yap Trench largely include magnetite, maghemite, and hematite. The maghemite dominates the sediment magnetic properties of the study area, and the sediment is more magnetic.

The magnetic particles of Yap Trench sediment are mostly pseudo single domains (PSD), and the hysteresis loop is mainly located within the range of 70%–90% of the SD+MD hybrid line.

The main sources of sediments in the Yap Trench are volcanic debris and nearly-source debris. The lower layers of Cores D148 and D149 are mainly volcanic debris transported by ocean currents; while the upper layers of Cores D149, D150, D151, and D152 are primarily nearly-source debris. The sediments are dominated by basalt and pyrozenite debris deposition near the trench caused by earthquakes and volcanic eruptions.

6 DATA AVAILABILITY STATEMENT

The data that support the findings of this study are available on request from the corresponding author.

7 ACKNOWLEDGMENT

The authors would like to thank Professor Wang Weiguo and Dr Liu Jianxing for providing insightful comments on this paper, and the anonymous reviewers for their constructive comments and helpful suggestions, which have improved the manuscript.

References

Arai K , Naruse H , Miura R , Kawamura K, Hino R, Ito Y, Inazu D, Yokokawa M, Izumi N, Murayama M, Kasaya T. 2013. Tsunami-generated turbidity current of the 2011 Tohoku-Oki earthquake. *Geology*, **41**(11): 1 195-1 198.

Borowski W S, Rodriguez N M, Paull C K, Ussler W. 2013. Are ^{34}S-enriched authigenic sulfide minerals a proxy for elevated methane flux and gas hydrates in the geologic record?. *Marine and Petroleum Geology*, **43**: 381-395.

Bridge J, Demicco R. 2011. Earth surface processes, landforms and sediment deposits. *Earth Surface Processes & Landforms*, **17**(1): 92-94.

Canfield D E, Olesen C A, Cox R P. 2006. Temperature and its control of isotope fractionation by a sulfate-reducing bacterium. *Geochimica et Cosmochimica Acta*, **70**(3): 548-561.

Day R, Fuller M, Schmidt V A. 1977. Hysteresis properties of titanomagnetites: Grain-size and compositional dependence. *Physics of the Earth and Planetary Interiors*, **13**(4): 260-267.

Dewangan P, Basavaiah N, Badesab F K, Usapkara A, Mazumdar A, Joshi R, Ramprasad T. 2013. Diagenesis of magnetic minerals in a gas hydrate/cold seep environment off the Krishna-Godavari basin, Bay of Bengal. *Marine Geology*, **340**: 57-70.

Dong Y, Li J H, Zhang W C, Zhang W Y, Zhao Y, Xiao T, Wu L F, Pan H M. 2016. The detection of magnetotactic bacteria in deep sea sediments from the east Pacific Manganese Nodule Province. *Environmental Microbiology Reports*, **8**(2): 239-249.

Dunlop D J, Özdemir Ö, Schmidt P. W. 1997. Paleomagnetism and paleothermometry of the Sydney Basin 2. Origin of an anomalously high unlocking temperature. *The Journal of Geophysical Research*: *Solid Earth*, **102**(B12): 27 285-27 295.

Dunlop D J, Özdemir Ö. 2001. Rock Magnetism: Fundamentals and Frontiers. Cambridge University Press, New York. p.1-573.

Dura T, Cisternas M, Horton B P, Ely L L, Nelson A R, Wesson R L, Pilarczyk J E. 2015. Coastal evidence for Holocene subduction-zone earthquakes and tsunamis in central Chile. *Quaternary Science Reviews*, **113**: 93-111.

Evans M E, Heler F. 2003. Environmental Magnetism. Principles and Applications of Enviromagnetics. Academic Press, San Diego. p.1-299.

Fujiwara T, Tamura C, Nishizawa A, Fujioka K, Kobayashi K, Iwabuchi Y. 2000. Morphology and tectonics of the Yap Trench. *Marine Geophysical Researches*, **21**(1-2): 69-86.

Gallo N D, Cameron J, Hardy K, Fryer P, Bartlett D H, Levin L A. 2015. Submersible- and lander-observed community patterns in the Mariana and New Britain trenches: Influence of productivity and depth on epibenthic and scavenging communities. *Deep Sea Research Part I*: *Oceanographic Research Papers*, **99**: 119-133.

Geissman J. 2004. Environmental magnetism: principles and applications of enviromagnetics. *Eos*, *Transactions American Geophysical Union*, **85**(20): 202.

Ghafarpour A, Khormali F, Balsam W, Karimi A, Ayoubi S. 2016. Climatic interpretation of loess-paleosol sequences at Mobarakabad and Aghband, Northern Iran. *Quaternary Research*, **86**(1): 95-109.

Guan H C, Zhu C, Zhu T X, Wu L, Li Y H. 2016. Grain size, magnetic susceptibility and geochemical characteristics of the loess in the Chaohu lake basin: Implications for the origin, palaeoclimatic change and provenance. *Journal of Asian Earth Sciences*, **117**: 170-183.

Jamieson A J, Fujii T, Solan M, Matsumoto A K, Bagley P M, Priede I G. 2009. First findings of decapod crustacea in the hadal zone. *Deep Sea Research Part I*: *Oceanographic Research Papers*, **56**(4): 641-647.

Jiang H. 2010. Dynamical mechanism and depositional responses of turbidity current sedimentation. *Oil & Gas Geology*, **31**(4): 428-435. (in Chinese with English abstract)

Kars M, Musgrave R J, Kodama K, Jonas A S, Bordiga M, Ruebsam W, Mleneck-Vautravers M J, Bauersachs T. 2017. Impact of climate change on the magnetic mineral assemblage in marine sediments from Izu rear arc, NW Pacific Ocean, over the last 1 Myr. *Palaeogeography*, *Palaeoclimatology*, *Palaeoecology*, **480**: 53-69.

Kawamura N, Kawamura K, Ishikawa N. 2008. Rock magnetic and geochemical analyses of surface sediment characteristics in deep ocean environments: A case study across the Ryukyu Trench. *Earth*, *Planets and Space*, **60**(3): 179-189.

Kim W, Doh S J, Yu Y, Lee Y L. 2013. Magnetic evaluation of sediment provenance in the northern East China Sea using fuzzy *c*-means cluster analysis. *Marine Geology*, **337**: 9-19.

Kirscher U, Winklhofer M, Hackl M, Bachtadse V. 2018. Detailed Jaramillo field reversals recorded in lake sediments from Armenia-Lower mantle influence on the magnetic field revisited. *Earth & Planetary Science Letters*, **484**: 124-134.

Kitahashi T, Jenkins R G, Nomaki H, Shimanaga M, Fujikura K, Kojima, S. 2014. Effect of the 2011 Tohoku Earthquake on deep-sea meiofaunal assemblages inhabiting the landward slope of the Japan Trench. *Marine Geology*, **358**: 128-137.

Kitajima H, Saffer D M. 2015. Consolidation state of incoming sediments to the Nankai Trough subduction zone: Implications for sediment deformation and properties. *Geochemistry*, *Geophysics*, *Geosystems*, **15**(7): 2 821-2 839.

Li B, Wang Y, Zhong H X, Zhang J Y, Li S, Li X J, Gao H F. 2016. Magnetic properties of turbidites in the Huatung Basin and their environmental implications. *Chinese Journal of Geophysics*, **59**(9): 3 330-3 342. (in Chinese with English abstract)

Li B, Li S, Wang Y, Zhang J Y, Li X J, Zhong H X, Tian C J. 2015. Magnetostratigraphy of core gx149 from the West Philippine Sea. *Marine Geology Frontiers*, **31**(8): 34-40. (in Chinese with English abstract)

Liu J, Zhu R X, Li T G, Li A C, Li J. 2007. Sediment magnetic signature of the mid-Holocene paleoenvironmental change in the central Okinawa Trough. *Marine Geology*, **239**(1-2): 19-31.

Liu Q, Banerjee S K, Jackson M J, Chen F H, Pan Y X, Zhu R X. 2003. An integrated study of the grain-size-dependent magnetic mineralogy of the Chinese loess/paleosol and its environmental significance. *Journal of Geophysical Research*, **108**(B9): 2 437.

Liu S M, Zhang W G, He Q, Li D J, Liu H, Yu L Z. 2010. Magnetic properties of East China Sea shelf sediments off the Yangtze Estuary: influence of provenance and particle size. *Geomorphology*, **119**(3-4): 212-220.

Lund S, Oppo D, Curry W. 2017. Late Quaternary paleomagnetic secular variation recorded in deep-sea sediments from the Demerara Rise, equatorial West Atlantic Ocean. *Physics of the Earth & Planetary Interiors*, **272**: 17-26.

Maher B A, Thompson R. 1999. Quaternary Climates, Environments and Magnetism. Cambridge University Press, Cambridge. p.390.

Meng Q Y, Li A C, Jing N, Xu Z K, Liu J G. 2006. Magnetostratigraphic and magnetic properties of marine sediments from the East Philippine Sea. *Marine Geology & Quaternary Geology*, **26**(3): 57-63. (in Chinese with English abstract)

Novosel I, Spence G D, Hyndman R D. 2005. Reduced magnetization produced by increased methane flux at a gas hydrate vent. *Marine Geology*, **216**(4): 265-274.

Oldfield F. 1994. Toward the discrimination of fine-grained ferrimagnets by magnetic measurements in lake and near-shore marine sediments. *Journal of Geophysical Research*: *Solid Earth*, **99**(B5): 9 045-9 050.

Pautot G, Nakamura K, Huchon P, Angelier J, Bourgois J, Fujioka K, Kanazawa T, Nakamura Y, Ogawa Y, Séguret M, Takeuchi A. 1987. Deep-sea submersible survey in the Suruga, Sagami and Japan Trenches: preliminary results of the 1985 Kaiko cruise, Leg 2. *Earth and Planetary Science Letters*, **83**(1-4): 300-312.

Prajith A, Rao V P, Kessarkar P M. 2015. Magnetic properties of sediments in cores from the Mandovi estuary, western India: Inferences on provenance and pollution. *Marine Pollution Bulletin*, **99**(1-2): 338-345.

Riisager P, Riisager J, Abrahamsen N, Waagstein R. 2002. New paleomagnetic pole and magnetostratigraphy of Faroe Islands flood volcanics, North Atlantic igneous province. *Earth and Planetary Science Letters*, **201**(2): 261-276.

Roza J, Jackson B, Heaton E, Negrini R. 2016. Paleomagnetic secular variation and environmental magnetism of Holocene-age sediments from Tulare Lake, CA. *Quaternary Research*, **85**(3): 391-398.

Sim M S, Bosak T, Ono S. 2011. Large sulfur isotope fractionation does not require disproportionation. *Science*, **333**(6038): 74-77.

Thompson R, Oldfield F. 1986. Environmental Magnetism. Allen & Unwin Press, Sydney. p.45.

Yang J C, Cui Z, Dada O A, Yang Y M, Yu H J, Xu Y, Lin Z L, Chen Y, Tang X. 2018. Distribution and enrichment of trace metals in surface marine sediments collected by the manned submersible Jiaolong in the Yap Trench, northwest Pacific Ocean. *Marine Pollution Bulletin*, **135**: 1 035-1 041.

Yang T, Dekkers M J, Zhang B. 2016. Seismic heating signatures in the Japan Trench subduction plate-boundary fault zone: evidence from a preliminary rock magnetic 'geothermometer'. *Geophysical Journal International*, **205**(1): 332-344.